New Dermatological Asymmetry Measure of Skin Lesions

Piotr Milczarski, Zofia Stawska
Faculty of Physics and Applied Informatics
University of Lodz
Pomorska str. 149/153, Lodz, Poland
{piotr.milczarski,zofia.stawska}@uni.lodz.pl

Łukasz Wąs, Sławomir Wiak
Institute of Mechatronics and Information Systems
Lodz University of Technology
Stefanowskiego str. 18/22, Lodz, Poland
{lukasz.was,slawomir.wiak}@p.lodz.pl

Marek Kot
Department of Dermatology and Venereology,
Medical University of Lodz
Haller Square1, 190-647 Lodz, Poland
{marek.kot}@umed.lodz.pl

Abstract—In the paper, we introduce a new dermatological asymmetry measure, *DASM*. We analyze and present dermatologists' approaches to melanocytic and non-melanocytic skin lesions. The asymmetry of skin lesion is described as a function of a shape, hue and structure. In the paper, the shape symmetry/asymmetry of the segmented skin lesion is discussed and a new dermatological measure is defined. The results of the method/algorithm using PH2 dataset are presented. Mild and malignant skin lesions are often very difficult to diagnose because there are many factors that can lead to misdiagnosis, which often leads to very long and expensive clinical treatment

Keywords—symmetry and asymmetry of skin lesion, dermatological asymmetry measure; dermatological features segmentation; skin lesions classification

I. Introduction

In the paper, we introduce a asymmetry measure of skin lesions that can be applied in dermatology.

Melanocytic and non-melanocytic skin lesions are often very difficult to recognize and diagnose [4][5]. Various sets of factors have to be taken into account so as to lead to proper diagnosis [4]. The proper dermatological diagnosis is based on clinical symptoms, experience of doctors and correct differentiation of skin lesions. Skin cancers may derive from the individual skin layers, the skin appendages, neurogenic blood, papilla and lymph derivatives [12][13]. One of the most difficult skin lesion to recognize is papilla which can vary in size, shape and appearance.

In our research, we focus on automated segmentation and classification lesion and features inside lesion. Fig. 1 presents general approach to the skin lesions processing and classification. To achieve the final prediction 3 stages are involved from the raw RGB dermoscopic image [16][42] and patient data:

Stage 1. Image processing to achieve lesions segmentation with their borders. Skin lesion is most often characterized by a texture or color different than in normal skin. Segmentation of lesions means finding lesions borders and it can be done by various well-known methods [19], [38]. Lesion segmentation is often very difficult problem depending on skin tone, aberrations, artifacts, lesion location etc. It is very important to take into account each of these factors [11], [15]. Many various segmentation method are used in this case e.g. histogram thresholding [14], [17], [18], clustering [25], [35], edge detection [1], probabilistic modeling [40]. A proper pre-processing steps are very important for the segmentation process [2], [34]. The methods and algorithms that can be used in filtering skin are presented in e.g. [26], [36]. Commonly, at the end of segmentation process, post-processing as region merging or peninsula removal is necessary [20].

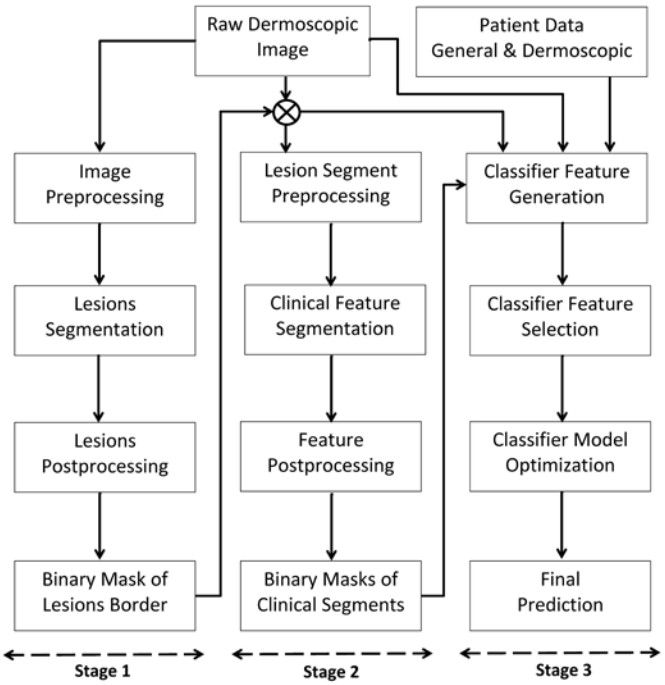

Fig. 1 The general approach to the skin lesions processing, segmentation and classification

Stage 2. Clinical feature segmentation [9] with resulting binary masks of clinical feature segments basing on the Stage1. Inside the image of skin lesion one can find multiple clinical features. Features may be global, local in the small area or can have multiple spots. Unlike lesion segmentation, each feature segmentation will have multiple segments. In skin lesion predicting [5] most commonly employed features are: streaks [27], [30], [31], pink shades [21], blotches [37], pigment network [32], blue-white veil [7]. These feature structures can also be categorized using their different patterns e.g. globular or homogeneous [33]. The main attributes used in clinical feature segmentation are hue/color, texture, structure, shape, location [10].

Stage 3. Final classification based on the feature selection and classifier model optimization taking Stage 1-2 into account as well as patient dermographic data [38], [39]. The raw images and dermographic data of the patient can be kept in a single or distributed database. Construction of classifier requires set of features characterizing the samples. Some features can be taken using dermoscopy images, but others have to be collected clinically. Final step is using this features in selected classification method. Commonly used classifiers are neural network [41], k-nearest neighbors [8], support vector machines [23] and ensemble learners [3].

In our research we use PH2 [24] and DermDB as the reference datasets. In the paper, we describe the part of the research that is finished at the Stage 3 in the point of classifier feature generation of shape asymmetry.

II. Dermatological And Dermoscopic Checklists

Skin is the largest organ in the human body. A physical examination of it without proper viewing is incomplete. The foundation of dermatological diagnosis is the ability to assess and differentiate correctly skin lesions. Sometimes, it is very difficult. In the case of primary skin eruptions, that are usually a direct result of the development of the skin disease in some cases, even in the early stage of the disease, we cannot find these efflorescence as they may occur for a short time.

Therefore, it is not surprising, that in many disorders of the internal organs, changes occur in the skin, which precise knowledge often facilitates the correct diagnosis [4].

Mild and malignant skin lesions are very often very difficult to diagnose. There are many factors that can lead to misdiagnosis which often leads to very long and expensive clinical treatment [13].

Melanocyte is a benign melanocytic proliferation. It can be either malignant malformation (hamartoma, a malignant tumor that is a developmental disorder) or acquired neoplasia. In the last case, not only the number of melanocytes has increased, but they are also (at least partially) nests or cords (strings) [6],[12],[29].

To correctly identify the lesion we need to assign specific methods for diagnosis of disease symptoms. Such methods are ABCD evaluation scale, 3-point checklist of dermoscopy (3PCLD) and 7-point checklist (7PCL).

Calculating asymmetry of shape, structures, and hue is one of the most important factors of correct diagnosis process of skin lesion [28]. In the paper, we focus on calculating asymmetry of shape. It is a starting point to asses asymmetry of the lesion because it is defined as asymmetry of shape, structures and hue.

Asymmetry occurs in methods for diagnosis such as ABCD evaluation scale, 3-point checklist of dermoscopy or 7-point checklist. We have carried out research concerning methods mentioned above. We have especially focused on 3-point checklist of dermoscopy and 7-point checklist.

TABLE I. 7- POINT CHECKLIST SCORING METHOD FOR DIAGNOSIS

Major ELM Criteria	**Score**
Atypical pigment network	2
Gray-blue areas	2
Atypical vascular pattern	2
Minor ELM Criteria	**Score**
Radial streaming (streaks)	1
Irregular diffuse pigmentation (blotches)	1
Irregular dots and globules	1
Regression structures	1

7-Point Checklist, 7PCL: a definition and histopathologic correlates of the 7 melanoma-specific dermoscopic criteria can be found in Tab. I.

3-point checklist of dermoscopy, 3PCLD is defined as:

- Asymmetry of shape, hue and structures in 1 or 2penperdiciular axes;
- Atypical pigment network with thickened lines and irregular distribution;
- Blue-white structures (veil) - any blue and/or white color within the lesion.

Two or more points suggest the diagnosis of atypical/malignant lesion.

The score for criterion presence is determined on the basis of the odds ratio. Odds ratios measure the capacity of each criterion of increasing the probability of a positive melanoma diagnosis. By simple addition of the criteria scores, a minimum total score of 3 is required for the diagnosis of melanoma

Odds ratios of each of the 7 criteria were calculated by multivariate analysis. 7-point score of 2 was given to the 3 criteria with odds ratios more than 5, and a score of 1 was given to the 4 criteria with odds ratios less than 5.

By simple addition of the individual scores a minimum total score of 3 is required for the diagnosis of melanoma, whereas a total score of less than 3 is indicative of a non-melanoma.

TABLE II 7-POINT CHECKLIST, 7PCL: DEFINITION AND HISTOPATHOLOGIC CORRELATES OF THE 7 MELANOMA-SPECIFIC DERMOSCOPIC CRITERIA

Criterion	Definition	Histopathologic correlates
1. Atypical pigment network	Black, brown, or gray network with irregular meshes and thick lines	Irregular and broadened rete ridges
2. Blue-whitish veil	Irregular, confluent, gray-blue to whitish-blue diffuse pigmentation	Acanthotic epidermis with focal hypergranulosis above sheets of heavily pigmented melanocytes in the dermis
3. Atypical vascular pattern	Linear-irregular or dotted vessels not clearly combined with regression structures	Neovascularization
4. Irregular streaks	Irregular, more or less confluent, linear structures not clearly combined with pigment network lines	Confluent junctional nests of melanocytes
5. Irregular pigmentation	Black, brown, and/or gray pigmented areas with irregular shape and/or distribution	Hyperpigmentation throughout the epidermis and/or upper dermis
6. Irregular dots/globules	Black, brown, and/or gray round to oval, variously sized structures irregularly distributed within the lesion	Pigment aggregates within stratum corneum, epidermis, dermo-epidermal junction, or papillary dermis
7. Regression structures	White areas (white scarlike areas) and blue areas (gray-blue areas, peppering, multiple blue-gray dots) may be associated, thus featuring so-called blue-whitish areas virtually indistinguishable from blue-whitish veil	Thickned papillary dermis with fibrosis and/or variable amounts of melanophages

III. DERMOSCOPIC DATABASES

Below we summarize briefly the accessible databases with images and their reference data on which we have conducted our research concerning asymmetry of shape, structures and hue.

The presented below databases are effects of a joint collaboration between hospitals, dermatology departments and IT institutions.

PH2 [24] contains 200 dermoscopic 8-bit RBG color images with a resolution of 768x560 pixels along with the corresponding medical annotations, comprising 80 common nevi, 80 atypical nevi, and 40 malignant melanomas acquired using a magnification of 20x under unchanged conditions.

DB [22] of Warsaw Memorial Cancer Center (Poland) 176 dermoscopic 8-bit JPEG color images with a resolution from 465x599 to 1077x1899 pixels along with the corresponding medical annotations, comprising 92 non-melanoma and 84 images of melanoma acquired using a dermoscope of the magnification of 20x.

DermBD dataset is an outcome of a joint collaboration between Department of Dermatology and Venereology of Medical University of Lodz, Institute of Mechatronics and Information Systems of Technical University of Lodz and Faculty of Physics and Applied Informatics of University of Lodz. DermDB database contains images with the reference data prepared and validated by expert dermatologists from Department of Dermatology and Venereology of Medical University in Lodz.

For each image in the DermDB database, the manual segmentation and the clinical diagnosis of the skin lesion as well as the identification of other important dermoscopic criteria are available. These dermoscopic criteria are based on 3-point checklist of dermoscopy and 7-point checklist. As the most important factor, we took into consideration oportunity of calculating asymmetry of shape, structures, and hue in process of skin lesion diagnosis process.

IV. DERMATOLOGICAL ASYMMETRY MEASURE, DASM

For the purpose of this article, we have introduced DASM – Dermatological Asymmetry Measure – integral asymmetry measure depending on shape, hue/color and structure.

In the above mentioned databases, especially PH2 the values for calculating asymmetry are given as follows encountered value 0 means fully symmetric, 1 means symmetric in 1 axes, 2 means fully asymmetric.

To achieve more precision we have proposed specific values to perform DASM (Dermatological Asymmetry Measure). These values are continuous and are described as follows:

- Shape < 0, 2 >
- Color/hue < 0, 2 >
- Structure < 0, 2 >

We have also increased the asymmetry count by adding the asymmetry of hue and structure. Our method predicts the asymmetry division into asymmetry of shape, hue/color and structure.

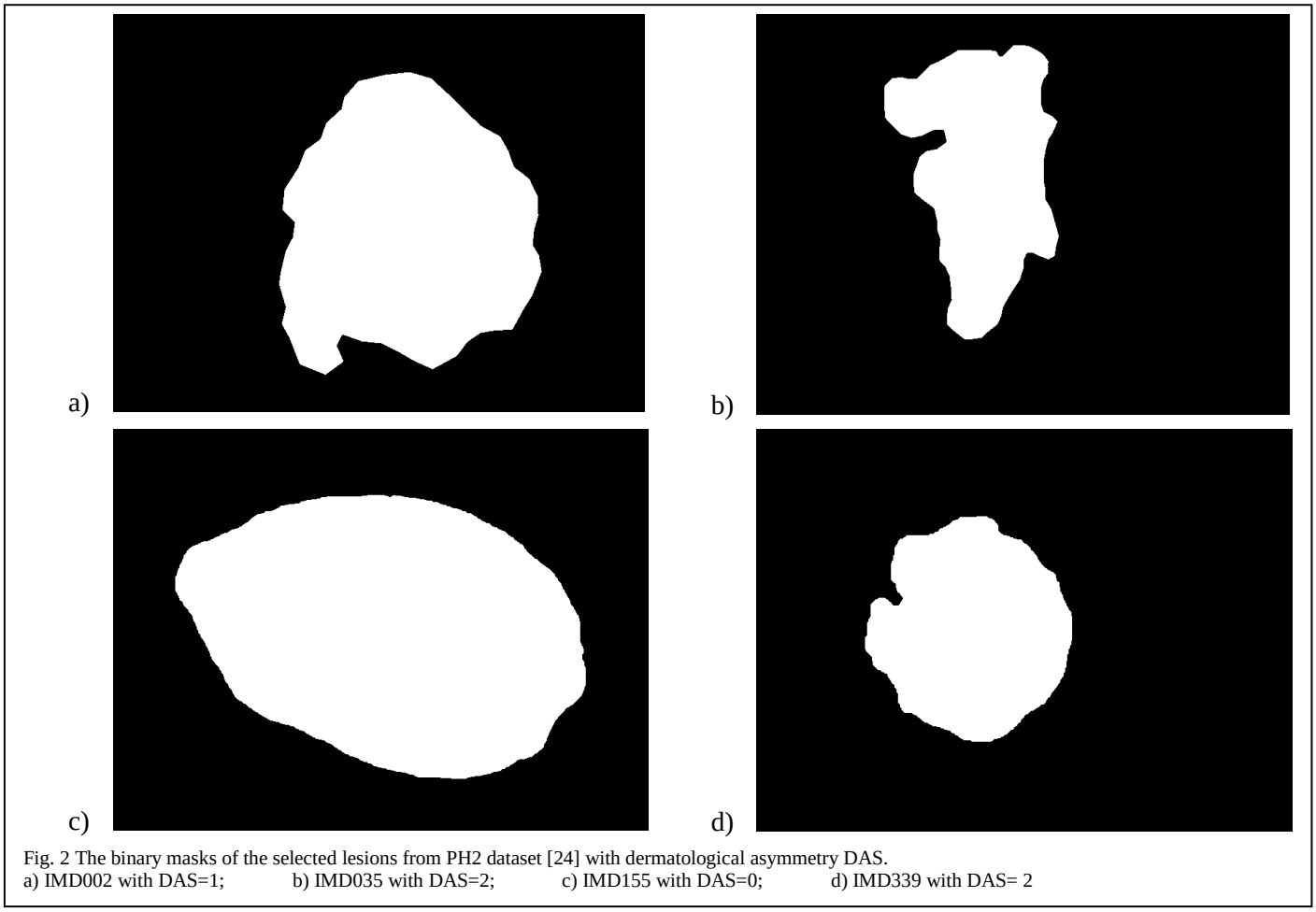

Fig. 2 The binary masks of the selected lesions from PH2 dataset [24] with dermatological asymmetry DAS.
a) IMD002 with DAS=1; b) IMD035 with DAS=2; c) IMD155 with DAS=0; d) IMD339 with DAS= 2

V. Dermatological Asymmetry Measure of Shape, DASMShape

After segmentation of the lesion and the features in the lesion, we have acquired binary masks, see Fig. 1. The next step is to select features for the classification of the lesion. We may use 3-point checklist or 7-point checklist. One of the features is asymmetry of the shape, hue and structure. Below, we present a new measure to estimate the asymmetry of the shape of the lesion. The shape in our case a shape of the lesion means a binary mask of the lesion. We propose the dermatological as a real value from <0,2>.

In the first step let us define:

- DAS – Dermatological Asymmetry, it is asymmetry of the shape, hue and structure. In dermatology, as we mentioned above, the value of the asymmetry can be: 0 for fully symmetric shapes; 1 for symmetric ones in one axis or 2 for asymmetric ones.
- DASM – Dermatological Asymmetry Measure – real asymmetry measure depending on shape, hue/color and structure;
- DASMShape – Dermatological Asymmetry Measure of Shape symmetry/asymmetry;
- DASMHue – Dermatological Asymmetry Measure of Hue/Color symmetry/asymmetry distribution;
- DASMStruct – Dermatological Asymmetry Measure of Structure symmetry/asymmetry distribution;
- GSSPT - a geometrical shape symmetry precision threshold of binary mask of the lesion is a threshold that after the axial transformation the original binary mask and mirror are the same in at least threshold value. PSSPT values are real values from <0,1>, e.g. 0.95 threshold means that the mirrored images are in 95% cover each other. The bigger the threshold the bigger similarity between mirrored images. The symmetry axis, SAx, depends on the GSSPT as well as the number of the symmetry axes for a given shape.
- NSA – number of symmetry axes depending on GSSPT.
- VoSS – a vector of shape symmetry, it as a vector which coefficients are equal to the number of symmetry axes.

Figures 2a-d show different binary masks for lesions with their corresponding dermatological asymmetry values assessed by the dermatology experts [24].

The method of deriving and estimating the new dermatological asymmetry measure value can be described as follows:

1. Calculate the number of symmetry axes for a given set of GSSPT thresholds $n(t_i)$, where t_i is a given threshold. After our experimental research we propose to choose the threshold values as a subset of a set of:

   {0.9, 0.91, 0.92, 0.93, 0.94, 0.95, 0.96, 0.97, 0.98}.

2. From the values of $n(t_i)$ construct a vector of shape symmetry (VoSS) **W**:

$$\mathbf{W} = [n(t_1), n(t_2),\ldots, n(t_k)] , \quad (1)$$

   where k≥2.

3. Design the DASMShape, Dermatological Asymmetry Measure of Shape, as a function of VoSS. Because the values of DASM and DASMShape are real value from <0,2> we propose positive, normalized to maximum value of 2 and continuous measure as an exponent of function depending of a VoSS vector:

$$\text{DASMShape} = 2 \exp (- f (\mathbf{W})) , \quad (2)$$

   where function $f: R^k \rightarrow R$.

VI. Results and Conclusions

In our experimental research we have tested several versions of function $f(\mathbf{W})$ in (2) and for a different subset of GSSPT thresholds. The smaller the number of thresholds the faster deriving of VoSS vector **W** defined as in (1). We have achieved the best results for the following subset of threshold values:

$$\{0.9, 0.93, 0.94, 0.95, 0.97\} \quad (3)$$

and function $f(\mathbf{W})$ defined as follows

$$f(W) = \sum_{i=5}^{5} a_i n_i^2 \quad (4)$$

where values $n(t)$ defined for (3) are $n_1 = n(t_1) = n(0.9), \ldots, n_5 = n(t_5) = n(0.95)$ and a vector of coefficients is defined as:

$$\mathbf{a}=[a_1, \ldots , a_5] = [0.004, 0.01, 0.17, 0.33, 0.5] \quad (5)$$

For the exemplary images in Fig. 2, the VoSS vectors **W** are presented in Tab. III. In the last left column, there are presented the values of the $f(\mathbf{W})$ function defined in (4) with the coefficients as in (5) with 6 digit accuracy.

TABLE III. THE EXPLAMPLES OF **W** VECTOR FOR IMAGES FROM PH2 DATASET

Image ID from PH2	VoSS vector W coefficient values					$f(\mathbf{W})$
	$n(0.9)$	$n(0.93)$	$n(0.94)$	$n(0.95)$	$n(0.97)$	
IMD002	1	0	0	0	0	1.992016
IMD035	8	3	3	1	0	0.226233
IMD155	2	2	2	2	1	0.155229
IMD339	12	12	7	6	0	0.000000

In Tab. IV it can be seen that the values of $f(\mathbf{W})$ function of the DASMShape measure do not always correspond with the values of the DAS values. The DAS values for the images presented in Tab. III are contained in the caption of Fig. 2.

In Tab. IV we present the classification results for the 167 cases from PH2 dataset out of 200. We excluded 33 of the cases because that images contain only part of the lesion. That is why in that cases asymmetry of their shape is impossible to derive automatically.

TABLE IV. RESULTS OF CLASSIFICATION FOR PH2 DATASET

DAS value PH2	Number of images with DAS	Number of misclassified images DASM		
		0	**1**	**2**
0	107		13	21
1	31	11		8
2	29	6	5	
Sum	167	17	18	29

After optimization of the thresholds we have achieved the lowest value of incorrectly classified images for the thresholds {0.971,1.532}. Overall sum of images with a given DAS value shows that in the PH2 dataset we have 107 cases with DAS lesion asymmetry equal 0. The proposed dermatological asymmetry measure DASMShape takes into account only one type of asymmetry. We cannot judge that symmetry in shape can give symmetry in hue or structure. It can be seen that for 6 cases from 29 with asymmetric lesions we achieved full symmetry in shape.

References

[1] Q. Abbas, M. E. Celebi, Irene Fondón García and M. Rashid, "Lesion border detection in dermoscopy images using dynamic programming," Skin Research and Technology, vol. 17, no. 1, pp. 91-100, 2011.

[2] Q. Abbas, I. F. Garcia, M. E. Celebi, W. Ahmad and Q. Mushtaq, "A perceptually oriented method for contrast enhancement and segmentation of dermoscopy images," Skin Research and Technology, vol. 19, no. 1, pp. 490-497, 2013.

[3] M. Abedini, Q. Chen, N. C. F. Codella, R. Garnavi and X. Sun, "Accurate and Scalable System for Automatic Detection of Malignant Melanoma," in Dermoscopy Image Analysis, M. E. Celebi, T. Mendonça and J. S. Marques, Eds., Boca Raton, CRC Press, 2015, pp. 293-343.

[4] G. Argenziano, G. Fabbrocini, P. Carli, V. De Giorgi, E. Sammarco, M. Delfino, "Epiluminescence microscopy for the diagnosis of doubtful melanocytic skin lesions. Comparison of the ABCD rule of dermatoscopy and a new 7-point checklist based on pattern analysis," Arch. Dermatol. 134, 15631570, 1998.

[5] G. Argenziano, H. P. Soyer, S. Chimenti, R. Talamini, R. Corona, F. Sera, M. Binder, L. Cerroni, G. De Rosa, G. Ferrara and R. Hofmann-Wellenhof, "Dermoscopy of pigmented skin lesions: results of a consensus meeting via the Internet," Journal of the American Academy of Dermatology, vol. 48, no. 9, pp. 679-693, 2003.

[6] G. Argenziano, H. P. Soyer, V. D. Giorgio, D. Piccolo, P. Carli, M. Delfino, A. Ferrari, R. Hofmann-Wellenhof, D. Massi, G. Mazzocchetti, M. Scalvenzi and I. H. Wolf, "Interactive atlas of

dermoscopy," Milan: Edra Medical Publishing & New Media, 2000.

[7] J. L. G. Arroyo, B. G. Zapirain and A. M. Zorrilla, "Blue-white veil and dark-red patch of pigment pattern recognition in dermoscopic images using machine-learning techniques," in IEEE International Symposium on In Signal Processing and Information Technology (ISSPIT), 2011, Bilbao, 2011, pp. 196-201.

[8] L. Ballerini, R. B. Fisher, B. Aldridge and J. Rees, "A color and texture based hierarchical K-NN approach to the classification of non-melanoma skin lesions," in Color Medical Image Analysis, M. E. Celebi and G. Schaefer, Eds., Netherlands, Springer, 2013, pp. 63-86.

[9] C. Barata, M. Ruela, M. Francisco, T. Mendonça and J. S. Marques, "Two systems for the detection of melanomas in dermoscopy images using texture and color features," IEEE Systems Journal, vol. 8, no. 3, pp. 965-979, 2014.

[10] M.H. Bharati, J.F. MacGregor, "Texture analysis of images using Principal Component Analysis," in: Proceedings of the SPIE - Process Imaging for Automatic Control, 4188, pp 27-33, 2001.

[11] F. Bogo, F. Peruch, A. B. Fortina and E. Peserico, "Where's the lesion? Variability in human and automated segmentation of dermoscopy images of melanocytic skin lesions," in Dermoscopy Image Analysis, M. E. Celebi, T. Mendonca and J. S. Marques, Eds., Boca Raton, CRC Press, 2015, pp. 67-96.

[12] R.N. Cardili, A.M. Roselino, "Elementary lesions in dermatological semiology," literature review. An Bras Dermatol. 91(5), 629-633, 2016.

[13] S. Chummun, N.R. McLean, "The management of malignant skin cancers," Surgery 29(10), 529-533, 2011.

[14] M. E. Celebi, Q. Wen, S. Hwang, H. Iyatomi and G. Schaefer, "Lesion border detection in dermoscopy images using ensembles of thresholding methods," Skin Research and Technology, vol. 19, no. 1, pp. e252-e258, 2013.

[15] M.E. Celebi, Q. Wen, H. Iyatomi, K. Shimizu, H. Zhou, G. Schaefer, "A state-of-the-art survey on lesion border detection in dermoscopy images," in: Dermoscopy Image Analysis, Celebi, M. E., Mendonca, T., Marques, J. S. (eds.), pp. 97-129. CRC Press, Boca Raton, 2015.

[16] T.M. Deserno, "Biomedical Image Processing," Springer, 2011.

[17] R. Garnavi, M. Aldeen, M. E. Celebi, G. Varigos and S. Finch, "Border detection in dermoscopy images using hybrid thresholding on optimized color channels," Computerized Medical Imaging and Graphics, vol. 35, no. 2, pp. 105-115, 2011.

[18] D.D. Gómez, C. Butakoff, B.K. Ersbll, W. Stoecker, "Independent histogram pursuit for segmentation of skin lesions," IEEE Transactions on Biomedical Imaging 55(1), 157-161, 2008.

[19] A.K. Jain, "Fundamental of Digital Image Processing," Prentice Hall of India, 2002.

[20] R. Kasmi, K. Mokrani, R. K. Rader, J. G. Cole and W. V. Stoecker, "Biologically inspired skin lesion segmentation using a geodesic active contour technique," Skin Research and Technology, vol. 0, no. 0, pp. 1-15, 2015.

[21] R. Kaur, P. P. Albano, J. G. Cole, J. Hagerty, R. W. LeAnder, R. H. Moss and W. V. Stoecker, "Real-time supervised detection of pink areas in dermoscopic images of melanoma: importance of color shades, texture and location," Skin Research and Technology, vol. 21, no. 4, pp. 466-473, 2015.

[22] M. Kruk, B. Swiderski, S. Osowski, J. Kurek, M. Slowinska, I. Walecka, "Melanoma recognition using extended set of descriptors and classifiers," J Image Video Proc. Vol 2015(1), Article:43, Dec 2015.

[23] J.J. Liu, M.H. Bharati, K.G. Dunn, J.F. MacGregor, "Automatic masking in multivariate image analysis using support vector machines," Chemometrics and Intelligent Laboratory Systems 79, 42-54, 2005.

[24] T. Mendonça, P.M. Ferreira, J.S. Marques, A.R.S. Marcal, J. Rozeira, "PH2 – A dermoscopic image database for research and benchmarking," in: 35th Annual International Conference of the IEEE Engineering in Medicine and Biology Society (EMBC), Osaka, pp. 5437-5440, 2013.

[25] M. Mete, S. Kockara and K. Aydin, "Fast density-based lesion detection in dermoscopy images," Computerized Medical Imaging and Graphics, vol. 35, no. 2, pp. 128-136, 2011.

[26] P. Milczarski, Z. Stawska, "Complex Colour Detection Methods Used In Skin Detection Systems," ISIM Vol.3 (1), 40-52, 2014.

[27] H. Mirzaalian, T. K. Lee and G. Hamarneh, "Learning features for streak detection in dermoscopic color images using localized radial flux of principal intensity curvature," in IEEE Workshop on In Mathematical Methods in Biomedical Image Analysis (MMBIA 2012), Breckenridge, 2012, pp. 97-101.

[28] C. Rosendahl, A. Cameron, I. McColl, D. Wilkinson, "Dermatoscopy in routine practice: 'Chaos and Clues'," Aust Fam Physician. 41(7), 482487, 2012.

[29] C. Rosendahl, P. Tschandl, A. Cameron, H. Kittler, "Diagnostic accuracy of dermatoscopy for melanocytic and nonmelanocytic pigmented lesions," J Am Acad Dermatol. 64(6), 10681073, 2011.

[30] M. Sadeghi, T. K. Lee, D. McLean, H. Lui and M. S. Atkins, "Detection and analysis of irregular streaks in dermoscopic images of skin lesions," IEEE Transactions on Medical Imaging, vol. 32, no. 5, pp. 849-861, 2013.

[31] M. Sadeghi, T. K. Lee, D. McLean, H. Lui and M. S. Atkins, "Oriented pattern analysis for streak detection in dermoscopy images," in Medical Image Computing and Computer-Assisted Intervention (MICCAI 2012), vol. 7510, Nice, Springer Berlin Heidelberg, 2012, pp. 298-306.

[32] M. Sadeghi, M. Razmara, T. K. Lee and M. S. Atkins, "A novel method for detection of pigment network in dermoscopic images using graphs," Computerized Medical Imaging and Graphics, vol. 35, no. 2, pp. 137-143, 2011.

[33] A. Saez, C. Serrano and B. Acha, "Global pattern classification in dermoscopic images," in Dermoscopy Image Analysis, M. E. Celebi, T. Mendonca and J. S. Marques, Eds., Boca Raton, CRC Press, 2015, pp. 183-209.

[34] G. Schaefer, M. I. Rajab, M. E. Celebi and H. Iyatomi, "Colour and contrast enhancement for improved skin lesion segmentation," Computerized Medical Imaging and Graphics, vol. 35, no. 2, pp. 99-104, 2011.

[35] P. Schmid, "Segmentation of digitized dermatoscopic images by two-dimensional color clustering," IEEE Transactions on Medical Imaging 18(2), 164-171, 1999.

[36] Z. Stawska, P. Milczarski, "Algorithms And Methods Used In Skin And Face Detection Suitable For Mobile Applications," ISIM, Vol.2 (3), 227-238, 2013.

[37] W. V. Stoecker, K. Gupta, R. J. Stanley, R. H. Moss and B. Shrestha, "Detection of asymmetric blotches (asymmetric structureless areas) in dermoscopy images of malignant melanoma using relative color," Skin Research and Technology, vol. 11, no. 3, pp. 179-184, 2005.

[38] P. Wighton, T.K. Lee, H. Lui, D.I. McLean, M.S. Atkins, "Generalizing common tasks in automated skin lesion diagnosis," IEEE Trans Inf Technol Biomed. 15, 622- 629, 2011.

[39] Ł. Wąs, M. Wyczechowski, S. Wiak, "Distributed Hierarchical Classification Grid with FCOC Coefficient," Logistyka, vol.4, 5061-5068, 2014.

[40] A. Wong, J. Scharcanski and P. Fieguth, "Automatic skin lesion segmentation via iterative stochastic region merging," IEEE Transactions on Information Technology in Biomedicine, vol. 15, no. 6, pp. 929-936, 2011.

[41] F. Xie, A. C. Bovik, "Automatic segmentation of dermoscopy images using self-generating neural networks seeded by genetic algorithm," Pattern Recognit. 46, 1012- 1019, 2013.

[42] H. Zare and M. T. B. Toossi, "Early detection of melanoma in dermoscopy of skin lesion images by computer vision based system," in Dermoscopy Image Analysis, M. E. Celebi, T. Mendonca and J. S. Marques, Eds., Boca Raton, CRC Press, 2015, pp. 345-384.